[Frontiers in Bioscience 14, 1283-1291, January 1, 2009]

Water transport in aquaporins: molecular dynamics simulations

Mitsunori Ikeguchi

Supramolecular Biology, International Graduate School of Arts and Sciences, Yokohama City University, 1-7-29, Suehiro-cho, Tsurumi-ku, Yokohama 230-0045, Japan

TABLE OF CONTENTS

1. ABSTRACT

Aquaporins and aquaglyceroporins are membrane channel proteins that selectively transport water and small molecules such as glycerol across biological membranes. Molecular dynamics simulations have made substantial contributions toward understanding the permeation mechanisms of aquaporins in atomic detail. Osmotic pressure is the driving force of the transport by aquaporins. The osmotic water permeability of aquaporins can be estimated from equilibrium molecular dynamics simulations by using linear response theory. The relationship between osmotic permeability and channel structure was investigated by the recently proposed p_f-matrix method. In addition to the water transport, other functions of aquaporins and aquaglyceroporins, i.e., glycerol permeation, proton blockage, and gating, have also been extensively studied by molecular dynamics simulations.

2. INTRODUCTION

Water is the most abundant substance in cells, accounting for approximately 70% of the total weight of a cell (1). Water plays crucial roles in many biological phenomena including protein folding and enzyme reactions. Because cell membranes are nearly impermeable to water, aquaporins, which are channel proteins embedded in membranes, facilitate and regulate water transport across cell membranes (2). Aquaporins are present in most life forms including bacteria, plants, and animals. In humans, more than ten different aquaporins have been identified, and defects in some aquaporins are associated with diseases.

The main feature of aquaporins is highly efficient water transport. The permeability of aquaporins is estimated to be ~10^9 water molecules per subunit per second. A second feature of aquaporins is the prevention of proton

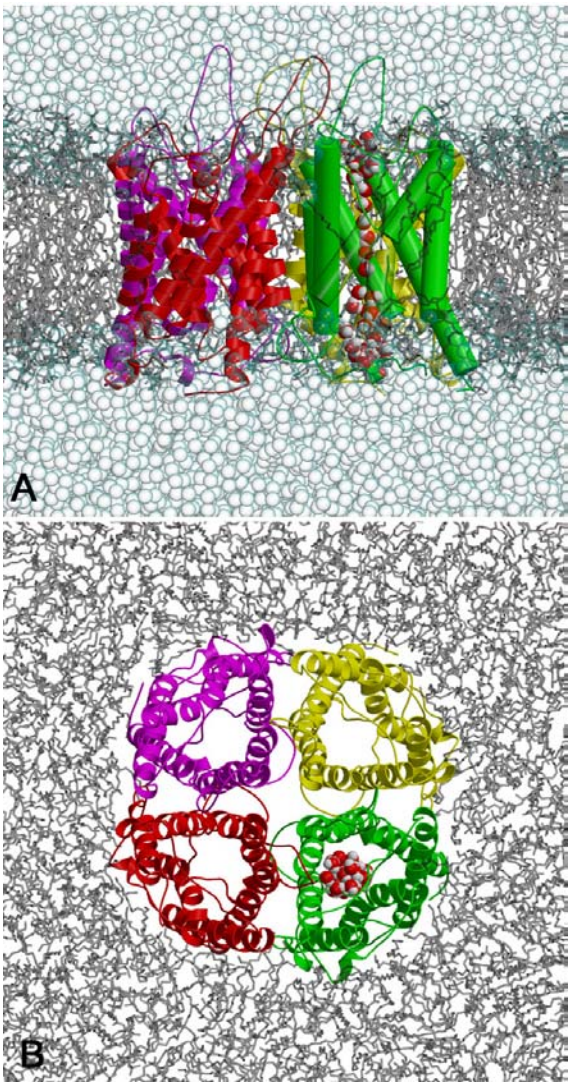

Figure 1. A setup of MD simulations for an aquaporin homotetramer embedded in membranes (20, 30). (A) Side view and (B) top view. Four monomers are colored in red, green, magenta, and yellow. Each monomer has an independent water pore, in which water molecules are displayed only for the green monomer. The pore water molecules form a single file inside the channel. Other than the water pores, the central pore, which is formed between the four monomers, has been proposed as a permeation route for ions and gases (52-54, 57).

permeation. Because pH is strictly regulated in cells, the leakage of protons may lead to severe cellular damage. Thus, it is critical that aquaporins block the leakage of protons, despite their highly efficient water-transport capability.

The aquaporin family contains two major subfamilies: the aquaglyceroporin subfamily, which transports small neutral molecules, e.g., glycerol, as well as water, and the aquaporin subfamily, which is characterized as being highly water selective. Three dimensional structures of aquaporins and aquaglyceroporins have been solved by using electron (3-6) and x-ray (7-12) crystallography. The overall structures of aquaporins and aquaglyceroporins are very similar: the root mean-square displacements for C-alpha atoms are 1.6–2.3 Å for the whole chain and 0.6–1.3 Å for the transmembrane helices. Notwithstanding the close similarity of overall structures among members of the aquaporin family, these proteins exhibit a rather wide range of permeability (13-19) due to subtle differences in side-chain structures of channel residues.

Molecular dynamics (MD) simulations have made substantial contributions toward understanding the permeation mechanisms of aquaporins and aquaglyceroporins. The present article reviews recent advances in MD simulations of aquaporins and aquaglyceroporins.

3. WATER TRANSPORT IN AQUAPORIN

Figure 1 shows the typical setup of MD simulations of aquaporins. All known structures of aquaporins and aquaglyceroporins are homotetramers, and each monomer has an independent water pore (Figure 1). The average radii of the channels during simulations were about the size of one water molecule (Figure 2B). As expected, an aquaglyceroporin member, GlpF, which is able to transport glycerols, has a larger channel radius than the other aquaporins that transport water only.

In the channel, there are two important regions acting as filters. The first filter is in the vicinity of the asparagine-proline-alanine (NPA) motif that is highly conserved in the aquaporin family. The NPA region is located at the center of the channel (Figure 2A). The second filter is the aromatic/arginine (ar/R) region, which is also called the selectivity filter (7). The ar/R region comprises the narrowest part in the channel (Figure 2A) and is located on the extracellular side of the channel.

The average water density profile within the channels (Figure 2C) (20) exhibits preferential sites for water: these sites are positions where water can form hydrogen bonds with residues in the inner surface of the channels. Water permeation through the channel occurs as a series of jumping motions between the preferential sites. The MD simulations revealed that protein-water interactions are the major interactions of water molecules in the NPA and ar/R regions, and that water-water interactions dominate in the other regions of the channel (21). Except for in the filter regions, neighboring water molecules form a hydrogen bond; thus, water molecules in the channel behave like a hydrogen-bonded wire (Figure 1).

Aquaporin AQP0, which is found in lens fiber cells of eyes, has unique features. First, AQP0 exhibits a much lower rate of water permeation than other aquaporins (16). Second, AQP0 forms not only water pores but also junctions between lens fiber cells (22). The three-dimensional structure of the AQP0-mediated membrane junction was determined by electron crystallography of double-layered two-dimensional crystals

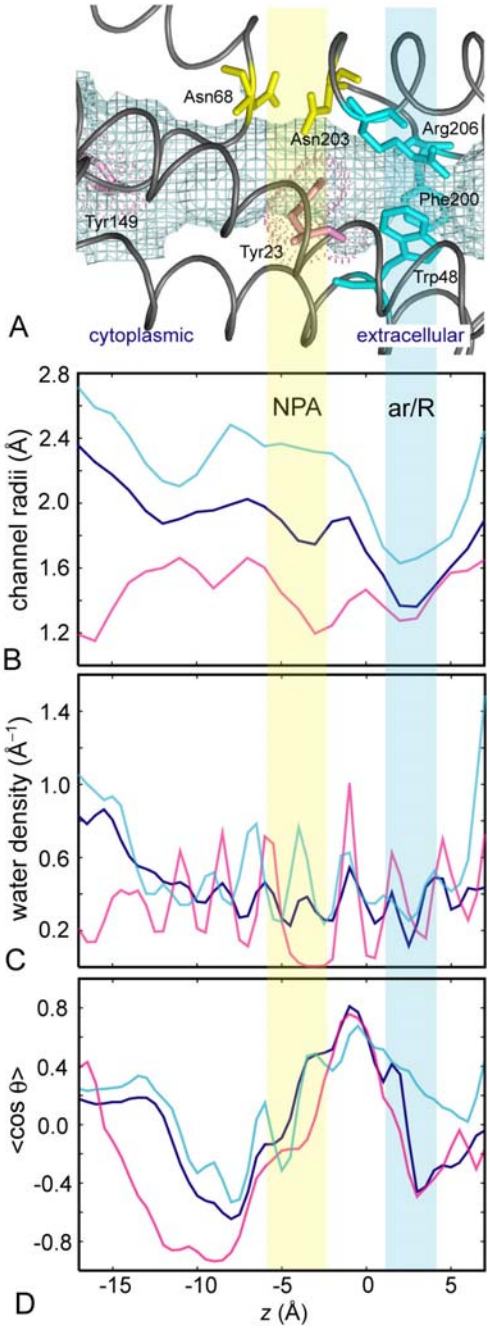

Figure 2. The channel structures and properties during MD simulations (20, 30). (A) The channel region of GlpF. The pore structure is represented by light-blue meshes. The NPA and the ar/R regions are colored in yellow and cyan, respectively. Tyr23 and Tyr149 of the superimposed AQP0 structure, which are shown in pink sticks and dot surfaces, protrude into the pore. The z-axis is aligned to the bilayer normal with the extracellular side on the right. (B) Average channel radii of GlpF (cyan), AqpZ (blue), and AQP0 (pink) in MD simulations. (C) Average number density of channel waters in MD simulations. (D) Average orientations of channel waters represented by the order parameter $\langle \cos\theta \rangle$, where θ is the angle between the dipole moment of water and the membrane normal.

(4, 5). The structure of the non-junctional AQP0 was also solved by x-ray crystallography of three-dimensional crystals (10). The water pores of the junctional AQP0 are critically narrower in several regions than those of other aquaporins, which led to the proposal that the junctional structure was a closed state of the channel. By contrast, the non-junctional structure was considered as an open state in which seven crystal water molecules were observed in the water pore (only three pore water molecules were found in the water pore of the junctional AQP0). However, even in the open structure of the non-junctional AQP0, the NPA region is occluded by Tyr23, a residue not seen in the other known aquaporin structures (see Figure 2A). MD simulations of the non-junctional AQP0 showed that the time average of the AQP0 channel radii were smaller than those of other aquaporins (Figure 2B) and, in particular, water density in the NPA region was almost absent (Figure 2C) (20). Nevertheless, during the simulations, a few water molecules could pass through the constricted region (Figure 3). This finding indicates that thermal fluctuations of critical side-chains play a crucial role in the water permeation through AQP0 (20, 23).

4. OSMOTIC PERMEABILITY

Because the transport of aquaporins is passive, the driving force of the transport is osmotic pressure. The osmotic water permeability of a single channel p_f, which characterizes the transport efficiency of aquaporins, is defined by:

$$p_f = j_w / \Delta C_s , \quad (1)$$

where j_w is the molar water flux of a channel and ΔC_s is the concentration difference of molecules between the two sides of the membrane. In MD simulations, the osmotic water permeability has been estimated by imposing explicit driving forces (24, 25). However, large driving forces are required to observe significant water permeation within the time scale of MD simulations. To avoid this problem, alternative approaches, in which the osmotic permeability, p_f, can be estimated from equilibrium MD simulations in the absence of a driving force, have been proposed, based on linear response theory (20, 26, 27) or Kramers-type theory (28, 29).

In the approach based on linear response theory (26), the configuration of channel water molecules is treated by the collective coordinate n, defined in differential form as:

$$dn = \sum_{k \in S(t)} dz_k / L , \quad (2)$$

where dz_k is the displacement of water k along the channel (aligned in the z direction), $S(t)$ is the set of water molecules in the channel, and L is the length of the channel. By this definition, the net amount of water permeation can be calculated by the time average of n. Every water molecule crossing the membrane through the channel from one side to

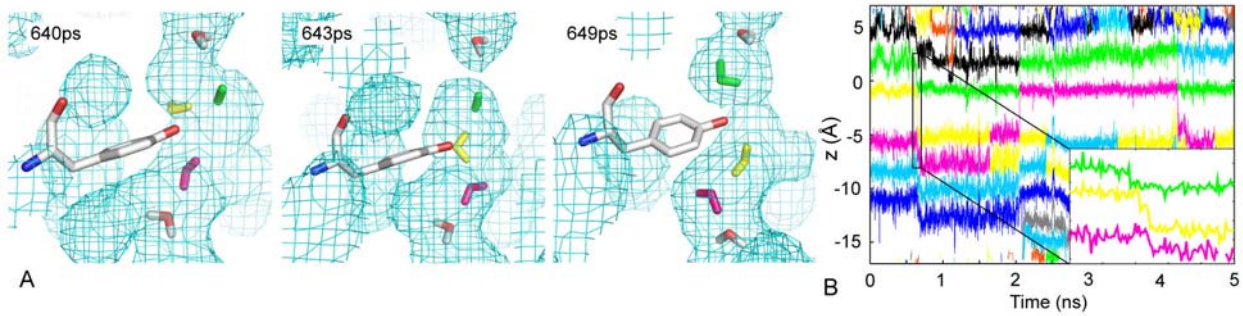

Figure 3. A water permeation process across the NPA region of AQP0 (20). (A) Snapshots in the MD simulations of AQP0. Tyr23 is illustrated by a stick model. Water molecules are colored in yellow, green, and pink. The yellow water molecule passed through the constriction region near Tyr23 in 9 ps. (B) Trajectories of water molecules in the channel. Colors of lines in the inset correspond to those of water molecules in the snapshots.

the other increases n by +1 (upward) or −1 (downward).

In the equilibrium simulations, the time average of n, $\langle n(t)\rangle_0$, becomes zero. However, the time average of n^2, $\langle n^2(t)\rangle_0$, is not zero, and behaves as the one-dimensional diffusion:

$$\langle n^2(t)\rangle_0 \approx 2D_n t + C \,, \tag{3}$$

where D_n is the diffusion coefficient, and C is a constant. The diffusion coefficient is related to the single-channel osmotic permeability constant p_f as follows:

$$p_f = v_w D_n \,, \tag{4}$$

where v_w is the volume of a single water molecule.

Although p_f calculated from simulations can be directly compared with the experimental value, a single quantity p_f does not explain in detail the contributions of each local channel region to water permeability. Therefore, the theory was extended to a form that explicitly describes the contributions from the local regions (30). The channel is subdivided into N subchannels with length L_N ($L = NL_N$). The collective coordinate, n_i, for subchannel i is defined as:

$$dn_i = \sum_{k \in S_i(t)} dz_k / L_N \,, \tag{5}$$

where $S_i(t)$ is the set of water molecules in subchannel i ($=1,\cdots,N$). Since $n = \sum_i n_i / N$, the mean square displacement of n becomes:

$$\langle n^2(t)\rangle_0 = \sum_{i,j} \langle n_i(t) n_j(t)\rangle_0 / N^2 \,, \tag{6}$$

where $\langle n_i(t) n_j(t)\rangle_0$ is written in a similar manner to Eq. (3), as:

$$\langle n_i(t) n_j(t)\rangle_0 \approx 2D_{ij} t + C \,. \tag{7}$$

The value of p_f is thus divided into the local contribution p_{ij} as follows:

$$p_f = \sum_{i,j} p_{ij} / N^2 \,, \tag{8}$$

with

$$p_{ij} = v_w D_{ij} \,. \tag{9}$$

We refer to the matrix of p_{ij} as the p_f matrix. Note that the diagonal element p_{ii} is the water permeability of subchannel i, and the off-diagonal element p_{ij} ($i \neq j$) denotes the covariance between the water molecules in i and those in j. It is convenient to convert the diagonal and off-diagonal elements p_{ij} into the correlation coefficient c_{ij}, defined as

$c_{ij} = p_{ij} \Big/ \left(p_{ii} p_{jj}\right)^{1/2}$. We refer to the matrix of c_{ij} as the p_f correlation matrix.

The most important feature of the p_f matrix is that the average of *all* the elements corresponding to the channel region, including both diagonal and off-diagonal elements, equals p_f (see Eq. 8). The formulation of the p_f matrix indicates that the correlated motions of widely separated water molecules influence osmotic permeability, as do adjacent water molecules.

Figure 4 shows the diagonal elements of p_f matrices and p_f correlation matrices for AqpZ, GlpF, and AQP0 (30). AqpZ, a highly water selective aquaporin found in *Escherichia coli*, showed high correlation for the entire channel. In the other aquaporins, clear reductions in c_{ij} for subchannels i and j separated by the NPA region were observed. In particular, AQP0, for which MD simulations were conducted in the non-junctional form, had almost no correlation across the NPA region due to no water density around the NPA region (Figure 4D). As described above, the elimination of water around the NPA region is caused by the occluding side chain of Tyr23 in AQP0 (see Figure 2A and C).

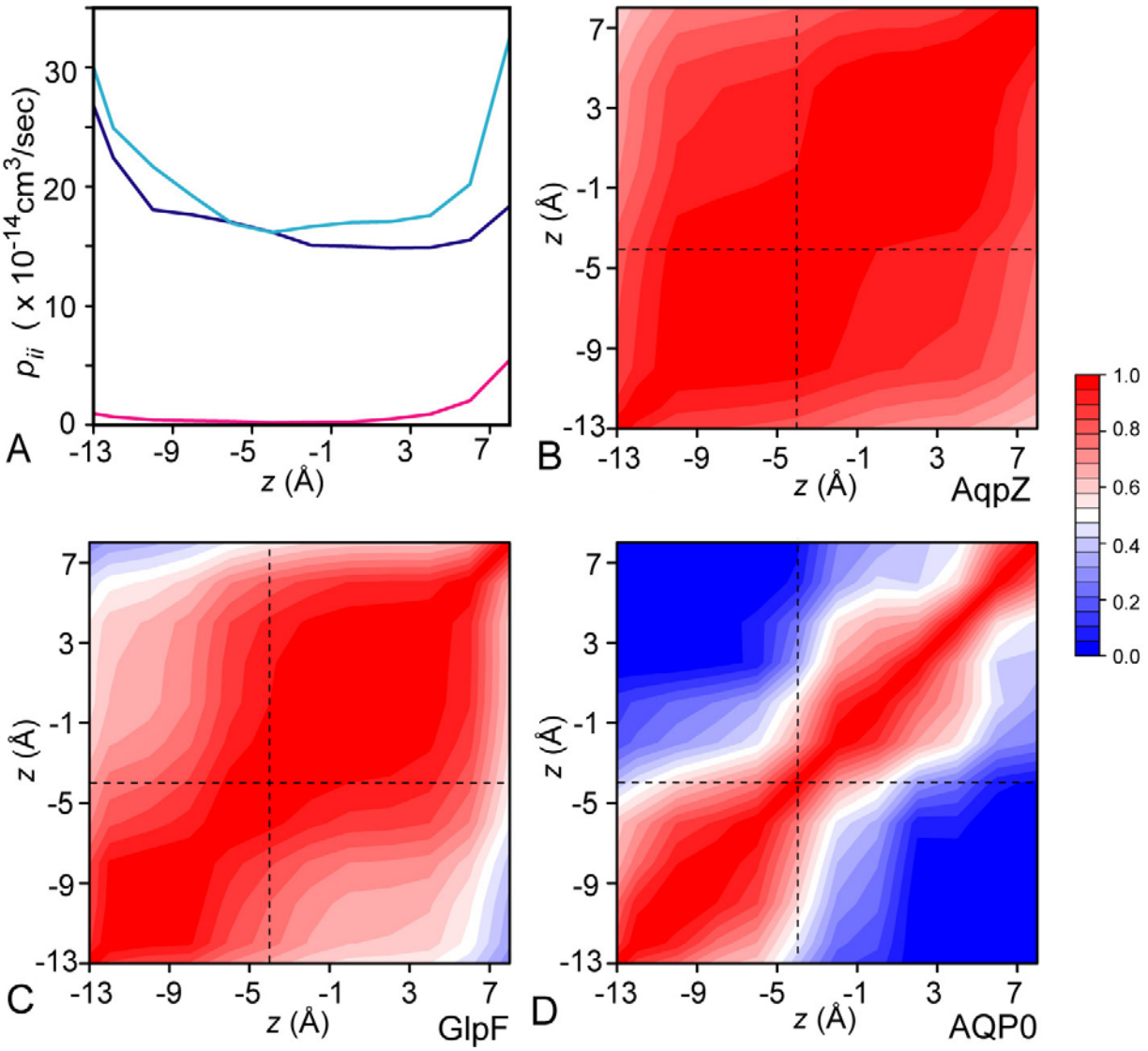

Figure 4. The p_f matrices for AqpZ, GlpF and AQP0 (30). (A) Diagonal elements p_{ii} of the p_f matrix for AqpZ (blue), GlpF (cyan), and AQP0 (pink). The p_f correlation matrices are shown for AqpZ (B), GlpF (C), and AQP0 (D). The broken lines indicate the position of the NPA region.

It is interesting to compare the p_f matrices of AqpZ, a pure water channel, and GlpF, a glycerol channel. In AqpZ, the strong correlation (i.e., the off-diagonal elements) largely contributed to the osmotic permeability (Figure 4B). In contrast, GlpF had weaker correlations than AqpZ (Figure 4C). Instead of the correlation, the diagonal elements p_{ii} of GlpF were larger than those of AqpZ (Figure 4A). The large pore size in GlpF (see Figure 2B) seems to increase the local permeability (i.e., the diagonal elements p_{ii}) and to decrease the correlation in water motion. As shown in Figure 2C, the water density in the pore of GlpF is significantly larger than that of AqpZ. Compared with the nearly ideal single-file water configuration in AqpZ, additional water molecules in the large pore of GlpF appear to break one-dimensional hydrogen bond networks of waters to reduce the correlation between the two ends of the channel.

A surprising feature of the p_f correlation matrices is that no significant reduction in correlation around the ar/R region was observed, even in the narrowest region of the channel (Figure 4). Instead of correlation, the diagonal elements were small around the ar/R region compared with those of other regions (Figure 4A), indicating that the local permeability around the ar/R region is low. This may be due to the strong interaction between the water and protein in the ar/R region. As discussed below, the ar/R region is responsible for the water selectivity of aquaporins.

The p_f matrix method revealed detailed differences in the permeation behavior of aquaporins. The p_f matrix method is an efficient and general way to analyze the osmotic permeation of water channels. This method is

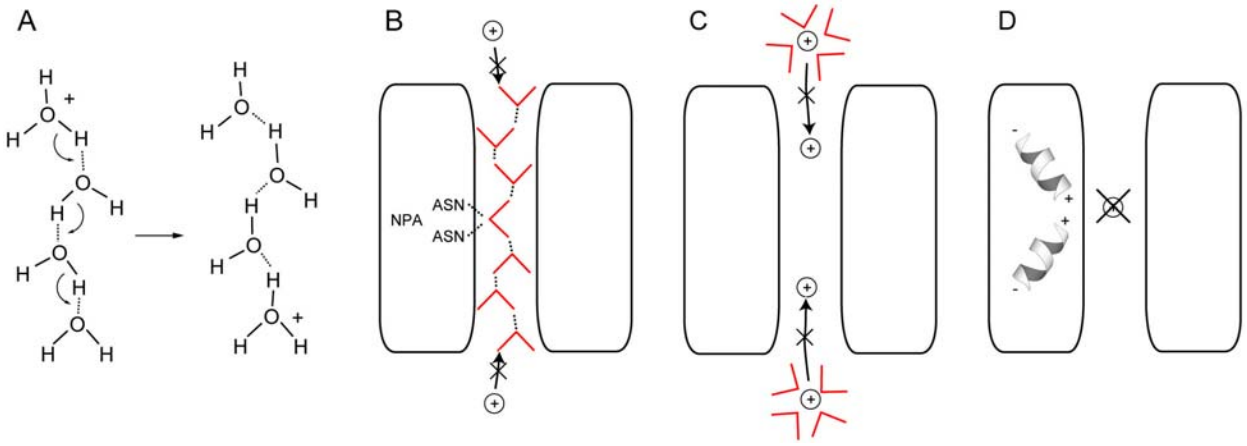

Figure 5. (A) The Grotthuss mechanism of proton transport. (B-D) Schematic representations of three explanations of proton blockage in aquaporins. (B) The bipolar water orientations observed in MD simulations prevent proton hopping via the Grotthuss mechanism (32-34). (C) Due to large dehydration penalty, the translocation of a proton from bulk water to the pore is accompanied by the large free-energy cost (35-37). (D) The electrostatic field generated mainly by the macrodipoles of alpha-helices in aquaporin is unfavorable for proton conduction (38-40).

applicable to other channel proteins or to artificial channels such as those in designed carbon nanotubes.

5. PROTON BLOCKAGE

In bulk water, protons can be conducted quickly through a chain of water molecules according to the Grotthuss mechanism (Figure 5A) (31). In the Grotthuss mechanism, protons hop from one water molecule to another water molecule via the rearrangement of covalent and hydrogen bonds. If water molecules in pores have the same orientation, the leakage of protons through the pores is permitted via the Grotthuss mechanism. How do aquaporins block the leakage of protons? Several simulations have been performed to address this question (21, 32-43). Three main explanations have been proposed so far. The first explanation is the bipolar water orientation (Figure 5B) (32-34), which has been observed in several simulations of aquaporins (Figure 2D) (20, 21, 32, 33). Water molecules are oriented in opposite directions with their hydrogen atoms pointing toward the exits. The asparagine residue in the NPA motif forms a hydrogen bond with a central water molecule, making its lone electron pairs unavailable as proton acceptors for the neighboring water molecules. Because proton hopping via the Grotthuss mechanism requires that each water molecule must be both a proton donor and acceptor for neighboring water molecules, the hydrogen bonding arrangement of the bipolar orientation inhibits proton conduction via the Grotthuss mechanism. The second explanation is the dehydration penalty for hydrated protons (Figure 5C) (35-37). Because bulk water is a highly polar environment and the aquaporin pore does not provide sufficient interactions for protons, the translocation of a proton from bulk water to the pore is accompanied by the large free-energy cost of the dehydration. The third explanation is that electrostatic interactions provided by aquaporins are unfavorable for proton conduction (Figure 5D) (38-40). The electrostatic barrier, generated mainly by the helical macrodipoles of alpha-helices in aquaporins, is responsible for the free-energy peak of the proton translocation near the NPA region. In addition, the electrostatic interactions of the ar/R region also contribute to the inhibition of proton conduction. These three explanations are related to each other. The electrostatic field generated by aquaporins is the main cause of the bipolar water orientation. The dehydration penalty is the balance between the hydration free energy and the interaction free energy in the pore including electrostatic contributions. Therefore, the cause of the proton blockage in aquaporins can be considered as the multiple related factors (31).

6. PERMEATION OF GLYCEROL AND OHTER MOLECULES

Aquaglyceroporins, which constitute a subfamily of the aquaporin family, facilitate small neutral molecules, e.g., glycerol, as well as water molecules. In contrast to water transport, the direct observation of complete glycerol permeation in conventional MD simulations is difficult because glycerol permeation has a longer time scale than typical current MD simulations (44). Instead of direct observations, free-energy approaches are often utilized to overcome the time-scale limitation of MD simulations (45). In the free-energy approaches, rare events are sampled by applying external forces. After the sampling, statistical mechanics procedures are used to remove the effects of external forces, and free-energy profiles can be constructed. In GlpF, a glycerol channel, free-energy profiles of glycerol permeation through the pore were calculated, employing Jarzynski's equation (46) or an adaptive biasing force approach (47). To investigate determinants of substrate selectivity in this channel, the free-energy profiles of glycerol permeation in AqpZ, a pure water channel, were also calculated and compared with those of GlpF (48). As expected, AqpZ has a much larger free-energy barrier than GlpF, indicating that AqpZ is impermeable to glycerol under normal conditions. In both AqpZ and GlpF, the free-energy barrier is located at the ar/R region, which may be primarily responsible for substrate selectivity.

Recently, comprehensive MD simulations investigating the selectivity mechanism of AQP1 and GlpF were reported (49). In this study, free-energy profiles for O_2, CO_2, NH_3, glycerol, urea and water through the water pores in AQP1 and GlpF were calculated using the umbrella sampling method. For small molecules permeating through AQP1, an anticorrelation between solute hydrophobicity and the free-energy barrier at the ar/R region was observed. Large molecules such as urea or glycerol were sterically excluded in AQP1 due to the small pore size at the ar/R region. Compared with AQP1, GlpF has the hydrophobic pocket opposite to the arginine at the ar/R region. Thus, GlpF allows hydrophobic solutes and comparatively large molecules to pass through the ar/R region, whereas AQP1 is impermeable to those molecules.

7. GATING

Gating is one of the fundamental functions of channels such as ion channels. Although most aquaporins are believed to be permanently open, some aquaporins exhibit gating in response to changes in conditions such as pH and phosphorylation (50). In bovine AQP0, water conductance is dependent on pH, with a maximum conductance at pH 6.5 and only about half of the maximum conductance at pH 7.5 (51). In a plant aquaporin, SoPIP2;1, phosphorylation of Ser115, which is located at the cytoplasmic side, triggers the channel opening (12). A drop in cytoplasmic pH, as well as dephosphorylation of Ser115, causes the channel closure of SoPIP2;1. MD simulations of SoPIP2;1 showed that, upon the phosphorylation, a cytoplasmic loop capping the channel in the closed state underwent large conformational changes, resulting in the opening of the water pore (12).

A gating motion of AqpZ was observed in MD simulations (27, 48). In the MD simulations, the sidechain of the highly conserved Arg189 at the ar/R region fluctuates between two distinct configurations denoted “up” and “down”. In the up configuration, the conformation of the sidechain of Arg189 is similar to that of other aquaporins, and the channel is open. In the down configuration, the sidechain of Arg189 occludes the pore in the ar/R region, leading that the channel is closed. In another x-ray structure of AqpZ derived from a different crystal form, two configurations of Arg189 corresponding to the open and closed states were also observed (11). In the x-ray structure, crystal packing appears to influence the preference of two configurations of Arg189. The possibility that protein-protein interactions may be involved in regulation of the gating was argued (11). However, the supporting functional evidence of gating of Arg189 has not been known yet. Its physiological significance, therefore, remains speculative (50).

8. SUMMARY AND PERSPECTIVE

Aquaporins are one of the most characterized channel proteins with atomic-resolution structural data. MD simulations have made substantial contributions to elucidating the mechanisms of water and glycerol permeation, proton blockage, and gating of aquaporins. New methodologies for understanding the mechanisms have also been developed to overcome limitations of MD simulations. In humans, more than ten different aquaporins are present, and some of these proteins may have functions other than the transport of water and glycerols (and small neutral molecules) through the water pores. For example, a secondary role of AQP0 has been proposed to be cell adhesion in lens fiber cells (2). The junctional structure of AQP0 was solved by using electron crystallography (4, 5). In addition to AQP0, the double-layered junctional structure was also determined for AQP4, suggesting that AQP4 also plays a role in cell adhesion (6). Stability of interlayer interactions is an intriguing issue for MD simulations.

Another pore, known as a central pore, is formed between the four monomers of aquaporins (see Figure 1B). The central pore has been proposed to be a permeation route of ions (52, 53) and gases (54). Gating for the central pore upon cGMP binding was also proposed (55, 56). Although MD simulations have contributed to the understanding of the functions of the central pore (53, 54), compared with the well-studied water pores, the central pore of aquaporins is still poorly understood. It remains an open question whether the central pore has any physiological importance (57). Aquaporins probably might not be a simple water pore. Computational approaches, as well as experimental approaches, will further shed light on many different functions of aquaporins.

9. ACKNOWLEDGMENTS

The author thanks Dr. Masanori Hashido and Prof. Akinori Kidera (Yokohama City University) for their collaboration on studies discussed in this article. These studies were supported in part by grants from the Ministry of Education, Science and Culture of Japan, as well as a grant from Japan Science and Technology Agency.

10. REFERENCES

1. B. Alberts, A. Johnson, J. Lewis, M. Raff, K. Roberts and P. Walter: Molecular biology of the cell. Garland Science, New York (2002)

2. S. Hohmann, S. Nielsen and P. Agre: Aquaporins. Academic Press, San Diego (2001)

3. K. Murata, K. Mitsuoka, T. Hirai, T. Walz, P. Agre, J. B. Heymann, A. Engel and Y. Fujiyoshi: Structural determinants of water permeation through aquaporin-1. *Nature* 407, 599-605 (2000)

4. T. Gonen, P. Sliz, J. Kistler, Y. Cheng and T. Walz: Aquaporin-0 membrane junctions reveal the structure of a closed water pore. *Nature* 429, 193-197 (2004)

5. T. Gonen, Y. Cheng, P. Sliz, Y. Hiroaki, Y. Fujiyoshi, S. C. Harrison and T. Walz: Lipid-protein interactions in double-layered two-dimensional AQP0 crystals. *Nature* 438, 633-638 (2005)

6. Y. Hiroaki, K. Tani, A. Kamegawa, N. Gyobu, K.

Nishikawa, H. Suzuki, T. Walz, S. Sasaki, K. Mitsuoka, K. Kimura, A. Mizoguchi and Y. Fujiyoshi: Implications of the aquaporin-4 structure on array formation and cell adhesion. *J Mol Biol* 355, 628-639 (2006)

7. D. Fu, A. Libson, L. J. Miercke, C. Weitzman, P. Nollert, J. Krucinski and R. M. Stroud: Structure of a glycerol-conducting channel and the basis for its selectivity. *Science* 290, 481-486 (2000)

8. H. Sui, B. G. Han, J. K. Lee, P. Walian and B. K. Jap: Structural basis of water-specific transport through the AQP1 water channel. *Nature* 414, 872-878 (2001)

9. D. F. Savage, P. F. Egea, Y. Robles-Colmenares, J. D. O'Connel, III and R. M. Stroud: Architecture and selectivity in aquaporins: 2.5 Å X-ray structure of aquaporin Z. *PLoS Biol* 1, 334-340 (2003)

10. W. E. C. Harries, D. Akhavan, L. J. W. Miercke, S. Khademi and R. M. Stroud: The channel architecture of aquaporin 0 at a 2.2-Å resolution. *Proc Natl Acad Sci USA* 101, 14045-14050 (2004)

11. J. Jiang, B. V. Daniels and D. Fu: Crystal structure of AqpZ tetramer reveals two distinct Arg-189 conformations associated with water permeation through the narrowest constriction of the water-conducting channel. *J Biol Chem* 281, 454-460 (2006)

12. S. Tornroth-Horsefield, Y. Wang, K. Hedfalk, U. Johanson, M. Karlsson, E. Tajkhorshid, R. Neutze and P. Kjellbom: Structural mechanism of plant aquaporin gating. *Nature* 439, 688-694 (2006)

13. M. L. Zeidel, S. V. Ambudkar, B. L. Smith and P. Agre: Reconstitution of functional water channels in liposomes containing purified red cell CHIP28 protein. *Biochemistry* 31, 7436-7440 (1992)

14. T. Walz, B. L. Smith, M. L. Zeidel, A. Engel and P. Agre: Biologically active two-demensional crystals of aquaporin CHIP. *J Biol Chem* 269, 1583-1586 (1994)

15. M. L. Zeidel, S. Nielsen, B. L. Smith, S. V. Ambudkar, A. B. Maunsbach and P. Agre: Ultrastructure, pharmacologic inhibition, and transport selectivity of aquaporin channel-forming integral protein in proteoliposomes. *Biochemistry* 33, 1606-1615 (1994)

16. B. Yang and A. S. Verkman: Water and glycerol permeabilities of aquaporins 1-5 and MIP determined quantitatively by expression of epitope-tagged constructs in *Xenopus oocytes*. *J Biol Chem* 272, 16140-16146 (1997)

17. M. J. Borgnia, D. Kozono, G. Calamita, P. C. Maloney and P. Agre: Functional reconstitution and characterization of AqpZ, the *E. coli* water channel protein. *J Mol Biol* 291, 1169-1179 (1999)

18. P. Pohl, S. M. Saparov, M. J. Borgnia and P. Agre: Highly selective water channel activity measured by voltage clamp: analysis of planar lipid bilayers reconstituted with purified AqpZ. *Proc Natl Acad Sci USA* 98, 9624-9629 (2001)

19. S. M. Saparov, S. P. Tsunoda and P. Pohl: Proton exclusion by an aquaglyceroprotein: a voltage clamp study. *Biol Cell* 97, 545-550 (2005)

20. M. Hashido, M. Ikeguchi and A. Kidera: Comparative simulations of aquaporin family: AQP1, AQPZ, AQP0 and GlpF. *FEBS Lett* 579, 5549-5552 (2005)

21. B. L. de Groot and H. Grubmüller: Water permeation across biological membranes: mechanism and dynamics of aquaporin-1 and GlpF. *Science* 294, 2353-2357 (2001)

22. D. Fotiadis, L. Hasler, D. J. Muller, H. Stahlberg, J. Kistler and A. Engel: Surface tongue-and-groove contours on lens MIP facilitate cell-to-cell adherence. *J Mol Biol* 300, 779-789 (2000)

23. B. G. Han, A. B. Guliaev, P. J. Walian and B. K. Jap: Water transport in AQP0 aquaporin: molecular dynamics studies. *J Mol Biol* 360, 285-296 (2006)

24. F. Zhu, E. Tajkhorshid and K. Schulten: Pressure-induced water transport in membrane channels studied by molecular dynamics. *Biophys J* 83, 154-160 (2002)

25. F. Zhu, E. Tajkhorshid and K. Schulten: Theory and simulation of water permeation in aquaporin-1. *Biophys J* 86, 50-57 (2004)

26. F. Zhu, E. Tajkhorshid and K. Schulten: Collective diffusion model for water permeation through microscopic channels. *Phys Rev Lett* 93, 224501 (2004)

27. M. Ø. Jensen and O. G. Mouritsen: Single-channel water permeabilities of *Escherichia coli* aquaporins AqpZ and GlpF. *Biophys J* 90, 2270-2284 (2006)

28. B. L. de Groot, D. P. Tieleman, P. Pohl and H. Grubmüller: Water permeation through gramicidin A: desformylation and the double helix: a molecular dynamics study. *Biophys J* 82, 2934-2942 (2002)

29. B. L. de Groot and H. Grubmüller: The dynamics and energetics of water permeation and proton exclusion in aquaporins. *Curr Opin Struct Biol* 15, 176-183 (2005)

30. M. Hashido, A. Kidera and M. Ikeguchi: Water transport in aquaporins: osmotic permeability matrix analysis of molecular dynamics simulations. *Biophys J* 93, 373-385 (2007)

31. J. M. Swanson, C. M. Maupin, H. Chen, M. K. Petersen, J. Xu, Y. Wu and G. A. Voth: Proton solvation and transport in aqueous and biomolecular systems: insights from computer simulations. *J Phys Chem B* 111, 4300-4314 (2007)

32. M. Ø. Jensen, E. Tajkhorshid and K. Schulten:

Electrostatic tuning of permeation and selectivity in aquaporin water channels. *Biophys J* 85, 2884-2899 (2003)

33. E. Tajkhorshid, P. Nollert, M. Ø. Jensen, L. J. W. Miercke, J. O'Connell, R. M. Stroud and K. Schulten: Control of the selectivity of the aquaporin water channel family by global orientational tuning. *Science* 296, 525-530 (2002)

34. B. Ilan, E. Tajkhorshid, K. Schulten and G. A. Voth: The mechanism of proton exclusion in aquaporin channels. *Proteins* 55, 223-228 (2004)

35. A. Burykin and A. Warshel: What really prevents proton transport through aquaporin? Charge self-energy versus proton wire proposals. *Biophys J* 85, 3696-3706 (2003)

36. A. Burykin and A. Warshel: On the origin of the electrostatic barrier for proton transport in aquaporin. *FEBS Lett* 570, 41-46 (2004)

37. M. Kato, A. V. Pisliakov and A. Warshel: The barrier for proton transport in aquaporins as a challenge for electrostatic models: the role of protein relaxation in mutational calculations. *Proteins* 64, 829-844 (2006)

38. B. L. de Groot, T. Frigato, V. Helms and H. Grubmüller: The mechanism of proton exclusion in the aquaporin-1 water channel. *J Mol Biol* 333, 279-293 (2003)

39. N. Chakrabarti, E. Tajkhorshid, B. Roux and R. Pomes: Molecular basis of proton blockage in aquaporins. *Structure* 12, 65-74 (2004)

40. N. Chakrabarti, B. Roux and R. Pomes: Structural determinants of proton blockage in aquaporins. *J Mol Biol* 343, 493-510 (2004)

41. M. Ø. Jensen, U. Rothlisberger and C. Rovira: Hydroxide and proton migration in aquaporins. *Biophys J* 89, 1744-1759 (2005)

42. H. Chen, Y. Wu and G. A. Voth: Origins of proton transport behavior from selectivity domain mutations of the aquaporin-1 channel. *Biophys J* 90, L73-75 (2006)

43. H. Chen, B. Ilan, Y. Wu, F. Zhu, K. Schulten and G. A. Voth: Charge delocalization in proton channels, I: the aquaporin channels and proton blockage. *Biophys J* 92, 46-60 (2007)

44. M. Ø. Jensen, E. Tajkhorshid and K. Schulten: The mechanism of glycerol conduction in aquaglyceroporins. *Structure* 9, 1083-1093 (2001)

45. C. Chipot and A. Pohorille: Free Energy Calculations. Springer, Berlin Heidelberg New York (2007)

46. M. Ø. Jensen, S. Park, E. Tajkhorshid and K. Schulten: Energetics of glycerol conduction through aquaglyceroporin GlpF. *Proc Natl Acad Sci USA* 99, 6731-6736 (2002)

47. J. Henin, E. Tajkhorshid, K. Schulten and C. Chipot: Diffusion of glycerol through Escherichia coli aquaglyceroporin GlpF. *Biophys J* 94, 832-839 (2008)

48. Y. Wang, K. Schulten and E. Tajkhorshid: What makes an aquaporin a glycerol channel? A comparative study of AqpZ and GlpF. *Structure* 13, 1107-1118 (2005)

49. J. S. Hub and B. L. de Groot: Mechanism of selectivity in aquaporins and aquaglyceroporins. *Proc Natl Acad Sci USA* 105, 1198-1203 (2008)

50. K. Hedfalk, S. Tornroth-Horsefield, M. Nyblom, U. Johanson, P. Kjellbom and R. Neutze: Aquaporin gating. *Curr Opin Struct Biol* 16, 447-456 (2006)

51. K. L. Nemeth-Cahalan, K. Kalman and J. E. Hall: Molecular basis of pH and Ca^{2+} regulation of aquaporin water permeability. *J Gen Physiol* 123, 573-580 (2004)

52. A. J. Yool and A. M. Weinstein: New roles for old holes: ion channel function in aquaporin-1. *News Physiol Sci* 17, 68-72 (2002)

53. J. Yu, A. J. Yool, K. Schulten and E. Tajkhorshid: Mechanism of gating and ion conductivity of a possible tetrameric pore in aquaporin-1. *Structure* 14, 1411-1423 (2006)

54. Y. Wang, J. Cohen, W. F. Boron, K. Schulten and E. Tajkhorshid: Exploring gas permeability of cellular membranes and membrane channels with molecular dynamics. *J Struct Biol* 157, 534-544 (2007)

55. T. L. Anthony, H. L. Brooks, D. Boassa, S. Leonov, G. M. Yanochko, J. W. Regan and A. J. Yool: Cloned human aquaporin-1 is a cyclic GMP-gated ion channel. *Mol Pharmacol* 57, 576-588 (2000)

56. S. M. Saparov, D. Kozono, U. Rothe, P. Agre and P. Pohl: Water and ion permeation of aquaporin-1 in planar lipid bilayers. Major differences in structural determinants and stoichiometry. *J Biol Chem* 276, 31515-31520 (2001)

57. Y. Wang and E. Tajkhorshid: Molecular mechanisms of conduction and selectivity in aquaporin water channels. *J Nutr* 137, 1509S-1515S (2007)

Abbreviations: MD: molecular dynamics; NPA: asparagine-proline-alanine; ar/R: aromatic/arginine

Key Words: Aquaporin, Water Transport, Osmotic Permeability, Molecular Dynamics Simulation, Review

Send correspondence to: Mitsunori Ikeguchi, Yokohama City University, 1-7-29, Suehiro-cho, Tsurumi-ku, Yokohama 230-0045, Japan, Tel: 81-45-508-7232, Fax: 81-45-508-7367, E-mail: ike@tsurumi.yokohama-cu.ac.jp

http://www.bioscience.org/current/vol14.htm